THE JOURNAL OF BIOLOGICAL CHEMISTRY VOL. 287, NO. 12, pp. 8746–8756, March 16, 2012

On Potential Interactions between Non-selective Cation Channel TRPM4 and Sulfonylurea Receptor SUR1*[S]

Received for publication, December 20, 2011, and in revised form, January 13, 2012 Published, JBC Papers in Press, January 30, 2012, DOI 10.1074/jbc.M111.336131

Monica Sala-Rabanal[‡], Shizhen Wang[‡§], and Colin G. Nichols[‡1]

From the [‡]Department of Cell Biology and Physiology and the Center for Investigation of Membrane Excitability Diseases, Washington University School of Medicine, St. Louis, Missouri 63110 and the [§]Department of Pharmacological and Physiological Sciences, St. Louis University, St. Louis, Missouri 63110

Background: SUR1, the regulatory subunit of K_{ATP} channels, was hypothesized to associate with TRPM4 to form novel channels, implicated in cell death following neurovascular trauma.
Results: The properties of heterologously expressed TRPM4 channels are not modified by SUR1.
Conclusion: The coupling between SUR1 and TRPM4 is unlikely.
Significance: The roles of TRPM4 and K_{ATP} channels in the pathogenesis of brain edema and hemorrhage should be reassessed.

The sulfonylurea receptor SUR1 associates with Kir6.2 or Kir6.1 to form K_{ATP} channels, which link metabolism to excitability in multiple cell types. The strong physical coupling of SUR1 with Kir6 subunits appears exclusive, but recent studies argue that SUR1 also modulates TRPM4, a member of the transient receptor potential family of non-selective cation channels. It has been reported that, following stroke, brain, or spinal cord injury, SUR1 is increased in neurovascular cells at the site of injury. This is accompanied by up-regulation of a non-selective cation conductance with TRPM4-like properties and apparently sensitive to sulfonylureas, leading to the postulation that post-traumatic non-selective cation currents are determined by TRPM4/SUR1 channels. To investigate the mechanistic hypothesis for the coupling between TRPM4 and SUR1, we performed electrophysiological and FRET studies in COSm6 cells expressing TRPM4 channels with or without SUR1. TRPM4-mediated currents were Ca^{2+}-activated, voltage-dependent, underwent desensitization, and were inhibited by ATP but were insensitive to glibenclamide and tolbutamide. These properties were not affected by cotransfection with SUR1. When the same SUR1 was cotransfected with Kir6.2, functional K_{ATP} channels were formed. In cells cotransfected with Kir6.2, SUR1, and TRPM4, we measured K_{ATP}-mediated K^+ currents and Ca^{2+}-activated, sulfonylurea-insensitive Na^+ currents in the same patch, further showing that SUR1 controls K_{ATP} channel activity but not TRPM4 channels. FRET signal between fluorophore-tagged TRPM4 subunits was similar to that between Kir6.2 and SUR1, whereas there was no detectable FRET efficiency between TRPM4 and SUR1. Our data suggest that functional or structural association of TRPM4 and SUR1 is unlikely.

The cation channel superfamily consists of a very large number of protein subunits, each of which contains one, two, or four pore-forming domains that interact in a tetrameric association to generate a mature transmembrane protein that surrounds a central ion conducting pathway (1). Depending on the detailed structure of the narrow selectivity filter, ion specificity of mature channels is variable, from highly specific for K^+, Na^+, or Ca^{2+}, to nonspecific for monovalent cations, to non-specifically permeable to any small organic and inorganic cations. The members of the transient receptor potential (TRP)[2] channel family are structurally similar to the voltage-gated K^+ (Kv) channels, each being formed as a tetramer of six-transmembrane (TM) helix subunits, each subunit containing a voltage sensor in TM4, and a pore-lining domain between TM5 and TM6 (see Fig. 1) (1). TRP channels are non-selective cation channels implicated in signal transduction, by means of Ca^{2+} permeation and/or membrane depolarization (2). They underlie many sensory and metabolic processes and are expressed in brain, tongue, pancreas, liver, adipose tissue, kidney, skeletal, and cardiac muscle and cells of the immune system, among others (2, 3). TRP channels are modulated by factors as diverse as voltage, Ca^{2+}, phosphoinositide 4,5-bisphosphate, diacylglycerol, mechanical stretch, and temperature (2, 4).

The ATP-binding cassette protein superfamily is encoded by one of the largest gene families in the mammalian genome (5). These proteins are all characterized by a core structure of two major six-TM domains each associated with a nucleotide binding fold (see Fig. 1*A*). The two nucleotide binding folds dimerize to generate two nucleotide binding sites at the interface, and nucleotide hydrolysis then provides the power stroke for activation of multiple processes. Typically, these involve the transport of specific substrates against a transmembrane gradient (5), but in two well studied systems, this involves the activation of electrodiffusive ion channels. In one of these, the cystic fibrosis transmembrane receptor, the channel is formed by the

* This work was supported, in whole or in part, by National Institutes of Health Grant HL95010 (to C. G. N.). This work was also supported by Postdoctoral Fellowship 10POST4280056 from the American Heart Association (to S. W.).
[S] This article contains supplemental Figs. S1 and S2.
[1] To whom correspondence should be addressed: Dept. of Cell Biology and Physiology, and Center for Investigation of Membrane Excitability Diseases, Washington University School of Medicine, 425 S. Euclid Ave., St. Louis, MO 63110. Tel.: 314-362-6630; Fax: 314-362-2244; E-mail: cnichols@wustl.edu.

[2] The abbreviations used are: TRP, transient receptor potential; TM, transmembrane; SUR, sulfonylurea receptor; K_{ATP}, ATP-sensitive K^+; NMG, *N*-methyl-D-glucamine; EGFP, enhanced green fluorescent protein; ECFP, enhanced cyan fluorescent protein; EYFP, enhanced yellow fluorescent protein.

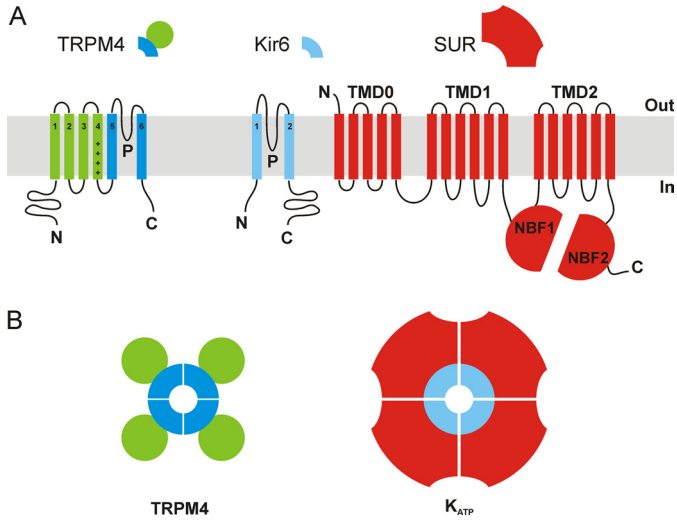

FIGURE 1. **Membrane topology models of TRPM4, Kir6, and SUR subunits (*A*) and predicted TRPM4 and K_{ATP} channel assembly (*B*).** *A*, TRPM4 monomers consist of six TM helices with a pore region (*P*) between TM5 and TM6, and a voltage sensor in TM4 (indicated by *plus signs*). Kir6 subunits contain only two TM segments linked by a pore-forming loop. SUR is composed of two interacting six-helix TM domains (TMD1 and TMD2), each followed by a nucleotide binding fold (*NBF1* and *2*); TMD0 interacts directly with Kir6 to translate agonist and antagonist binding events into a gating signal. *B*, functional TRPM4 channels are formed by oligomerization of four TRPM4 subunits. The pore-lining helices are surrounded by the voltage-sensing S1–S4 helices. In K_{ATP} channels, four Kir6 subunits couple to determine the channel pore, and each Kir6 subunit is associated with one SUR subunit, and the pore-lining helices are surrounded by the SUR subunits.

transmembrane segments of the ATP-binding cassette protein itself (6). In the other, the ATP-sensitive K^+ (K_{ATP}) channel, the sulfonylurea receptor (SUR) is physically and functionally coupled to one of two members of the inward-rectifying K^+ (Kir) family of cation channels, Kir6.1 or Kir6.2 (see Fig. 1*A*), with each Kir6 subunit associated with one SUR subunit (Fig. 1*B*) (7). One study reported that SUR1 may regulate another Kir channel subunit, Kir1.1 (8), but the claim remains controversial, and the strong physical interaction of SUR1 with Kir6.2 appears to be specific and exclusive.

However, a series of recent studies have developed the hypothesis that SUR1 also associates with and regulates the activity of TRPM4, a member of the melastatin subfamily of TRP channels (9). These channels are structurally distant from the Kir family, but intriguingly, TRPM4, similar to Kir6.2, is sensitive to inhibition by cytoplasmic ATP in the micromolar range (10). It has been reported that, after traumatic brain or spinal cord injury, or ischemia after stroke, SUR1 is up-regulated in neurovascular cells such as reactive astrocytes and endothelial cells at the site of injury (11, 12). In parallel, there is a dramatic up-regulation of a non-selective cation conductance that has recently been suggested to underlie the brain edema and secondary hemorrhage that often follow and contribute to the devastating effects of stroke, brain, or spinal cord trauma (13). This conductance has been characterized as non-selective for monovalent cations, Ca^{2+}-activated but Ca^{2+}-impermeable, and ATP-sensitive (11, 14), these properties being very reminiscent of those exhibited by TRPM4 channels studied in recombinant cell lines (15, 16). In addition, this conductance appears to be reduced by sulfonylurea drugs such as glibenclamide, and enhanced in the presence of the SUR1-specific K_{ATP} channel opener diazoxide (11). These observations have led to the postulation that post-traumatic nonspecific cationic currents are determined by SUR1-modulated TRPM4 channel complexes (9, 13). Consistent with this hypothesis is the observation that secondary hemorrhage following spinal cord injury is ameliorated by administration of glibenclamide, and in both $SUR1^{-/-}$ and $TRPM4^{-/-}$ mice (17, 18).

Despite these correlations, direct evidence for functional or structural association between TRPM4 and SUR1 is lacking. To address this important deficit, in the present study, we examined the properties of TRPM4 channels in the absence and presence of SUR1 subunits in COSm6 cells, by means of inside-out membrane patch clamping and FRET.

EXPERIMENTAL PROCEDURES

Heterologous Expression—COSm6 cells were plated on coverslips in six-well plates and cultured in Dulbecco's modified Eagle's medium (Invitrogen) supplemented with 10% fetal bovine serum, 10^5 units/liter penicillin, and 100 mg/liter streptomycin. At 60% confluency, cells were transfected with the relevant plasmids using FuGENE 6 transfection reagent (Roche Diagnostics) at a 1 μg of DNA to 3 μl of FuGENE ratio, and the amount of DNA per well was kept constant at 2 μg. Multiple transfections were made in parallel.

Electrophysiology—For most experiments (Figs. 2–4), cells were either transfected with 1) mouse TRPM4b (the long splice variant of TRPM4 in pEGFP-N1, hereafter referred to as TRPM4); 2) empty pEGFP vector (GFP, or mock-transfected); 3) equal amounts of TRPM4 and GFP; or 4) equal amounts of TRPM4 and hamster SUR1 in pECE (SUR1). The same SUR1 DNA was cotransfected with mouse Kir6.2 (in pEGFP) for K_{ATP} channel expression, at a 1:0.6 ratio (see Fig. 5). For experiments entailing coexpression of K_{ATP} and TRPM4 subunits (see Fig. 6), the transfection mixture contained SUR1, Kir6.2 and GFP (K_{ATP}) or SUR1, Kir6.2 and TRPM4 (K_{ATP} + TRPM4) at a 1:0.6:1 ratio. Cells expressing the different EGFP fusion proteins fluoresced under ultraviolet light and were selected for patch clamp analysis. Experiments were performed at room temperature 24–72 h after transfection using a chamber that allowed rapid changes between four different solutions as described (19). Micropipettes were prepared from nonheparinized hematocrit glass (Kimble-Chase) on a horizontal puller (Sutter Instrument) and filled to a typical electrode resistance of 1.5 megohms with pipette solution containing 140 mM NaCl, 10 mM KCl, 1 mM $MgCl_2$, 5 mM $CaCl_2$, and 10 mM Hepes (pH adjusted to 7.4 with NaOH). The composition of the different experimental bath solutions is given in the figure legends. Unless otherwise noted, all buffers were adjusted to pH 7.4 with NaOH. 100 mM stocks of glibenclamide, tolbutamide, and diazoxide (in dimethyl sulfoxide), or K^+-ATP (in a 150 mM KCl solution, with the pH adjusted to 7.4 with KOH), were kept at −20 °C and diluted into working concentrations immediately before use. All chemicals were purchased from Sigma. Membrane patches were voltage-clamped using an Axopatch 1D amplifier (Molecular Devices), and currents were recorded at 0 mV or +100 mV (pipette voltage, −100 mV) in on-cell or inside-out excised patch configuration. In other experiments, a pulse protocol was applied in which membrane potential (V_m)

was held at 0 mV for 50 ms and stepped to a test value for 500 ms before returning to the holding potential for an additional 150 ms. The test potential varied from −100 to +100 mV in 20-mV increments. Currents were measured at the end of the 500-ms voltage pulse. Data were filtered at 2 kHz, and signals were digitized at 5 kHz with a Digidata 1322A (Molecular Devices). pClamp and Axoscope software (Molecular Devices) was used for pulse protocol application and data acquisition.

Macroscopic $^{86}Rb^+$ Efflux Assays—GFP-transfected cells and cells cotransfected with Kir6.2 and SUR1 were pre-incubated

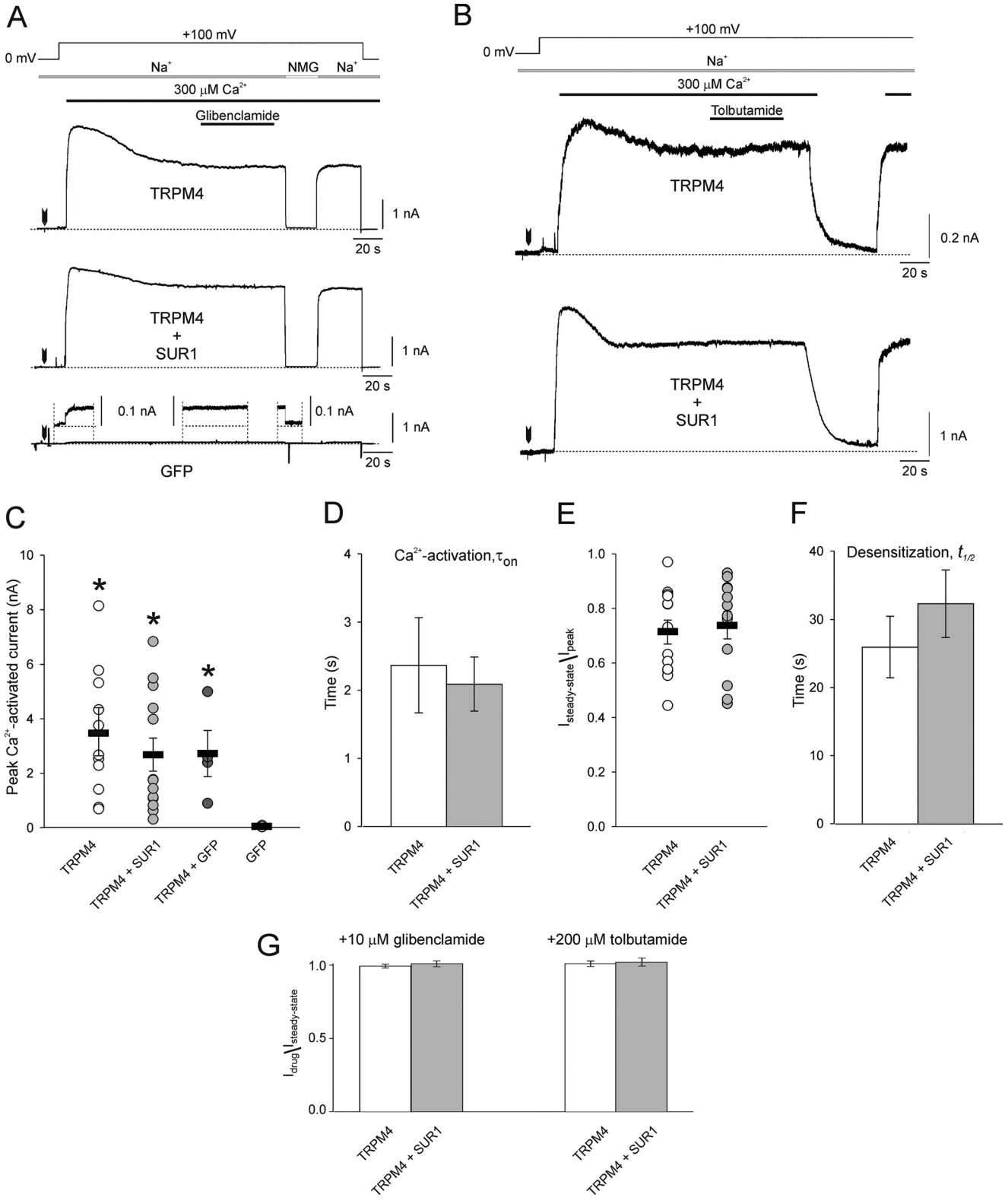

for 6 h in culture medium containing 1 μCi/ml ^{86}RbCl (PerkinElmer Life Sciences), and then incubated for 30 min in Ringer's solution containing 118 mM NaCl, 2.5 mM $CaCl_2$, 1.2 mM KH_2PO_4, 4.7 mM KCl, 25 mM $NaHCO_3$, 1.2 mM $MgSO_4$, and 10 mM Hepes (pH 7.4); plus metabolic inhibitors, *i.e.* 2.5 μg/ml oligomycin and 1 mM 2-deoxy-D-glucose (Sigma). Subsequently, at selected time points, the medium was collected and replaced with fresh solution, in the absence or presence of 10 μM glibenclamide from the same batch as that used in the experiments described above. Upon completion of the assay, cells were lysed with 2% SDS and collected, and radioactivity in the samples was measured by liquid scintillation. Raw data are shown as $^{86}Rb^+$ efflux relative to total counts, including all time points and the cell lysate. To estimate the rate constants for K_{ATP}-dependent $^{86}Rb^+$ efflux k_2, flux data were fitted to Equation 1,

$$\text{Relative efflux} = 1 - \exp[-(k_1 + k_2) \times \text{time}] \quad \text{(Eq. 1)}$$

where the apparent rate constants for nonspecific efflux k_1 were obtained from mock-transfected cells, assuming $k_2 = 0$.

FRET—TRPM4-ECFP and TRPM4-EYFP fusion constructs were generated by subcloning the TRPM4 cDNA into pECFP-N1 or pEYFP-N1 (Clontech), using the SalI and SacII restriction sites; SUR1 cDNA was inserted into pEYFP-N1 between the EcoRI and AgeI sites to generate SUR1-EYFP; and Kir6.2-ECFP was constructed by means of overlapping PCR, as described (20). COSm6 cells were cultured as above and transfected with 1) TRPM4-ECFP, 2) TRPM4-EYFP, 3) Kir6.2-ECFP, or 4) SUR1-EYFP; equal amounts of 5) TRPM4-ECFP and TRPM4-EYFP or 6) TRPM4-ECFP and SUR1-EYFP; or 7) Kir6.2-ECFP and SUR1-EYFP at a 1:0.6 ratio. ECFP/EYFP-based FRET studies were conducted as reported (21). Briefly, cells were incubated for 48–60 h after transfection to reach full confluency and then thoroughly washed with PBS and harvested. Data were acquired with a QuantaMaster fluorescence spectrofluorometer (Photon Technology International); ECFP or EYFP fusion proteins were excited at 430 or 480 nm, and fluorescence emission spectra from 450–550 nm and 490–550 nm, respectively, were collected. Background cellular fluorescence was obtained from untransfected cells and subtracted from the total fluorescence in transfected cells. The FRET efficiencies were calculated using Equation 2,

$$E = \frac{F_{430(525)} - F^{CFP}_{430(525)}}{F_{480(525)}} \quad \text{(Eq. 2)}$$

where $F_{430(525)}$ and $F_{480(525)}$ are the emissions at 525 nm following excitation at 430 nm and 480 nm, respectively, and F^{CFP} is the emission at 525 nm of cells transfected with ECFP fusion constructs.

Data Analysis—Data were analyzed using Clampfit (version 10.1, Molecular Devices) and Excel (Microsoft). SigmaPlot 10.0 (Systat Software) and CorelDRAW X3 13.0 (Corel Corp.) were used for curve fitting, statistics, and figure preparation. Results are presented as mean ± S.E. Where indicated, one-way analysis of variance and Kruskal-Wallis test, paired or unpaired Student's *t* test, were applied to evaluate statistical differences between groups.

RESULTS

Properties of TRPM4 Channels Expressed in COSm6 Cells Are Not Altered by Coexpression with SUR1—Figs. 2–4 summarize the essential biophysical properties of TRPM4 channels expressed heterologously in COSm6 cells alone (when applicable, *white symbols* and *bars*) and cotransfected with SUR1 subunits (*gray symbols* and *bars*). In experiments shown in Fig. 2, membrane potential (V_m) was first held at 0 mV, and patches were excised into a Ca^{2+}-free Na^+ buffer before V_m was stepped to +100 mV (see representative traces in Fig. 2, *A* and *B*). In TRPM4 and TRPM4 + SUR1, currents on cell and in inside-out excised patches in absence of intracellular Ca^{2+} were indistinguishable from those measured in mock-transfected GFP cells (Fig. 2*A*, *bottom panel*), *e.g.* 0.013 ± 0.002 nA on cell, and 0.024 ± 0.003 nA in excised patches at +100 mV (n = 8 each). When the internal surface of the patch was exposed to 300 μM Ca^{2+}, outward currents in TRPM4-transfected cells were activated rapidly (Fig. 2, *A* and *B*) and peaked at 3.4 ± 0.7 nA (Fig. 2*C*); individual current measurements varied from 0.7 to 8 nA but were at least 15-fold higher than in GFP cells (0.05 ± 0.01 nA; Fig. 2*C*, *black symbols*). The activation time constant τ_{on} was 2.4 ± 0.7 s (Fig. 2*D*). In cells cotransfected with TRPM4 and SUR1, Ca^{2+}-activated currents peaked at 2.7 ± 0.7 nA (Fig. 2*C*; $p = 0.43$ when compared with TRPM4 cells, unpaired Student's *t* test), with τ_{on} = 2.1 ± 0.4 s (Fig. 2*D*; $p = 0.72$). Although not significantly different, peak currents in TRPM4 + SUR1 were on average 20% smaller than in TRPM4

FIGURE 2. **TRPM4-mediated Na^+ currents are Ca^{2+}-activated, undergo desensitization, and are insensitive to sulfonylureas, and these properties are not altered by cotransfection with SUR1.** *A* and *B*, continuous current traces from representative cells transfected with mouse TRPM4b (*TRPM4*), equal amounts of TRPM4 and hamster SUR1 (*TRPM4 + SUR1*), or empty pEGFP vector (*GFP*). V_m was held initially at 0 mV and outward currents (represented by *upward deflections*; the *dotted lines* indicate zero current) were recorded on cell and in inside-out excised patches exposed to Ca^{2+}-free Na^+ buffer (*Na^+*) containing 150 mM NaCl, 1 mM $MgCl_2$, and 10 mM Hepes; *arrowheads* mark the point of excision. Subsequently, V_m was stepped to +100 mV and, upon current stabilization, the patch was exposed to Na^+ buffer in presence of 300 μM $CaCl_2$ (*i.e.* 300 μM free Ca^{2+}). After Ca^{2+}-activated currents in TRPM4 and TRPM4 + SUR1 had decayed to a steady-state (desensitization), patches were exposed for at least 1 min to 10 μM glibenclamide (*A*) or 200 μM tolbutamide (*B*). In *A*, background currents were obtained by exposing the patch to NMG buffer containing 150 mM NMG, 1 mM $MgCl_2$, 0.3 mM $CaCl_2$, and 10 mM Hepes (pH 7.4 with Tris); and in *B*, by exposing the patch to Ca^{2+}-free Na^+ buffer. *C*, peak Ca^{2+}-activated Na^+ currents in all experimental groups, plus in patches from cells transfected with equal amounts of TRPM4 and GFP (*TRPM4 + GFP*). *Circles* represent data from individual patches (n = 6–12); *bars* indicate the means ± S.E. of all experiments. *, $p < 0.05$ as compared with the GFP-transfected cells (one-way analysis of variance and Kruskal-Wallis test). *D*, time constant τ_{on} of Ca^{2+}-dependent activation in TRPM4 (*white bars*) and TRPM4 + SUR1 (*gray bars*), estimated by fitting the time course of peak current activation to a single exponential relationship. Data are means ± S.E. of 12 experiments per transfection type. *E*, desensitized, steady-state Ca^{2+}-activated currents ($I_{steady\text{-}state}$), normalized to the peak (I_{peak}) in each individual experiment. Data are represented as in *C*. *F*, estimated half-time $t_{1/2}$ of current desensitization. Data are represented as in *D*. *G*, steady-state current after exposure to 10 μM glibenclamide (*left*, from experiments as in *A*) or 200 μM tolbutamide (*right*, from experiments as in *B*) (I_{drug}), normalized to the current in absence of drug ($I_{steady\text{-}state}$) in each individual experiment. Data are represented as in *D* and *F*. Glibenclamide experiments, n = 8; tolbutamide experiments, n = 5. *C–G*, no significant differences were found between TRPM4 and TRPM4 + SUR1 for any of the parameters studied (p = 0.4–0.8; unpaired Student's *t* test).

(Fig. 2*C*) but were virtually identical to those measured in cells cotransfected with equal amounts of TRPM4 and empty vector, *i.e.* TRPM4 + GFP (Fig. 2*C*, *dark gray symbols*). This suggests that the moderate reduction in current observed in TRPM4 + SUR1 patches is due to the cells being transfected with half the amount of TRPM4 DNA than TRPM4 cells, rather than to a possible sequestering effect of SUR1. Shortly after peaking, Ca^{2+}-activated currents in TRPM4 and TRPM4 + SUR1 began to decrease until they reached a steady-state, in a type of inactivation known as desensitization that has been well characterized in TRPM4 channels, as reviewed (16). As shown in Fig. 2*E*, the extent of desensitization was variable, but on average, currents decreased 29 ± 4% in TRPM4 and 26 ± 5% in TRPM4 + SUR1 ($p = 0.71$), with half-times $t_{1/2}$ estimated at 26 ± 5 s in TRPM4 and 32 ± 5 s in TRPM4 + SUR1 (Fig. 2*F*; $p = 0.39$). There was no inhibition of steady-state TRPM4 currents by glibenclamide or tolbutamide, either in the absence or presence of SUR1 (Fig. 2, *A*, *B*, and *G*), but in all cases, currents were reduced reversibly to background levels when intracellular Na^+ was replaced with *N*-methyl-D-glucamine (NMG; Fig. 2*A*) or in Ca^{2+}-free Na^+ buffer (Fig. 2*B*; see also Fig. 4*A*). In mock-transfected cells, small background currents (~0.1 nA) were activated in the presence of Ca^{2+}; these remained stable throughout the experiment, were not affected by glibenclamide (Fig. 2*A*, *bottom panel*) or tolbutamide (see for example Fig. 6*A*, *bottom*), were blocked by NMG (Fig. 2*A*, *bottom*), and inactivated in the absence of Ca^{2+} (see Fig. 6*A*, *bottom*).

We then investigated the voltage dependence of currents (Fig. 3) by applying a series of V_m steps in excised patches from TRPM4 and TRPM4 + SUR1 cells (−100 to +100 mV in 20-mV increments; Fig. 3*A*). In TRPM4 alone patches (Fig. 3*A*, *left panels*), currents in absence of Ca^{2+} (Fig. 3*A*, *panel 1*, *left*; and Fig. *3B*, *white triangles*) were small and not different from those recorded in mock-transfected cells (data not shown). Ca^{2+}-dependent currents, presented here at the steady-state after desensitization (Fig. *3A*, *panel 2*, *left*), showed slow activation at positive potentials, fast deactivation at negative potentials, and outward rectification (Fig. *3B*, *white circles*), as described (22, 23). Replacement of Na^+ with NMG resulted in current block, especially at positive potentials (Fig. 3*A*, *panel 4*, *left*; and Fig. *3B*, *white squares*). Coexpression with SUR1 did not alter these properties (Fig. 3*A*, *right panels*). As shown in Fig. 3*B*, the voltage dependence of background currents (*triangles*), steady-state Ca^{2+}-activated Na^+ currents (*circles*), and NMG block (*squares*) was identical in TRPM4 (*white symbols*) and TRPM4 + SUR1 (*gray symbols*). At all voltages tested, Ca^{2+}-activated steady-state currents were insensitive to glibenclamide, both in TRPM4 (Fig. 3*A*, *panel 3*, *left*; and Fig. 3*C*) and TRPM4 + SUR1 (Fig. 3*A*, *panel 3*, *right*; and Fig. 3*D*).

In the next series of experiments, presented in Fig. 4, patches from TRPM4 and TRPM4 + SUR1 cells were excised as usual in a Ca^{2+}-free solution, and outward currents were activated at +100 mV by exposure to 300 μM Ca^{2+} (representative data shown in Fig. 4*A*). After desensitization, we tested the effect of 10 μM free ATP, as reported (10). Steady-state currents were significantly inhibited by ATP (Fig. 4*A*), but the extent of inhibition was again similar in TRPM4 and TRPM4 + SUR1 (Fig. 4*B*), respectively 41 ± 4% and 50 ± 4% in ($p = 0.13$). The time constant of ATP inhibition τ_{ATP}, best estimated by fitting the time course of current decay to a single exponential relationship, was 1.8 ± 0.2 s in TRPM4 and 2.3 ± 0.4 in TRPM4 + SUR1 ($n = 6$ each; $p = 0.1$). The K_{ATP} channel opener diazoxide did not counter this inhibition, instead, in both cases, it increased it slightly and reversibly by ~10%. Currents recovered 80–95% upon removal of ATP (Fig. 4, *A* and *B*, *washout*); inactivated in Ca^{2+}-free buffer (Fig. 4, *A* and *B*, *background*) with similar kinetics, *i.e.* $\tau_{off} = 14 \pm 2$ s in TRPM4 and 9 ± 3 s in TRPM4 + SUR1 ($p = 0.3$); and reactivated again upon re-exposure to Ca^{2+} (Fig. 4*A*).

Same SUR1 Subunits Form Functional K_{ATP} Channels—To validate the SUR1 cDNA used in all previous experiments, we cotransfected it with Kir6.2; the properties of the resulting K_{ATP} channels are summarized in Fig. 5. When the same voltage pulse protocol as in Fig. 3 was applied on-cell to patches from cells cotransfected with Kir6.2 and SUR1 (Fig. 5*A*, *top left*), we observed that currents were small and undistinguishable from those measured in mock-transfected cells (Fig. 5*A*, *bottom left*). Voltage-dependent K^+ currents of up to 4 nA rapidly activated upon excision into a Ca^{2+}-free, 150 mM K^+ buffer (Fig. 5*B*, *top right*). Accordingly, K_{ATP} channels are inhibited by intracellular ATP, and spontaneously open when their cytoplasmic side is exposed to an ATP-free solution (7). In GFP-transfected cells, excision into K^+ buffer did not elicit any significant current (Fig. 5*B*, *bottom right*). Data from five K_{ATP} channel-expressing cells were normalized as described in the legend and represented in Fig. 5*B* as means ± S.E.; note that, in our experimental conditions, *i.e.* $[K^+]_{out} = 10$ mM and $[K^+]_{in} = 150$ mM, K_{ATP}-mediated K^+ currents reversed very close to E_K (−68 mV) (Fig. 5*B*, *circles*). In other experiments (Fig. 5, *C* and *D*), exposure of cells cotransfected with Kir6.2 and SUR1 to metabolic inhibitors (oligomycin and 2-deoxy-D-glucose) led to the activation of time-dependent $^{86}Rb^+$ efflux that was 1) severalfold higher than in mock-transfected cells and 2) significantly inhibited by glibenclamide (Fig. 5*C*), *i.e.* the rate of K_{ATP}-specific $^{86}Rb^+$ efflux k_2, proportional to the K_{ATP}-mediated K^+ conductance, dropped 90% in presence of the drug (Fig. 5*D*). Again, this was consistent with the well understood properties of cloned K_{ATP} channels (7, 24, 25).

When Expressed in Same Cells, SUR1 Subunits Control Kir6.2 Channel Activity, without Modifying TRPM4 Channel Properties—In experiments shown in Fig. 6 (see representative traces in Fig. 6*A*), patches from cells transfected with Kir6.2 and SUR1 (K_{ATP}), Kir6.2, SUR1, and TRPM4 (K_{ATP} + TRPM4), or mock-transfected (GFP), were first held at 0 mV and excised into a Ca^{2+}-free, K^+ buffer. In K_{ATP} and K_{ATP} + TRPM4, this elicited instantaneous outward K_{ATP} currents, 0.45 ± 0.09 nA in K_{ATP} ($n = 5$) and 0.23 ± 0.04 nA in K_{ATP} + TRPM4 ($n = 12$; $p < 0.05$); individual measurements varied (Fig. 6*B*) but were at least 10-fold higher than in mock-transfected cells (0.02 ± 0.001 nA; $n = 5$). Subsequently, the patches were exposed to a Na^+ buffer, and this abolished the K_{ATP} currents (Fig. 6*A*). Then, the voltage was stepped to +100 mV, and the patches were exposed to 300 μM Ca^{2+}, which induced small outward currents in both K_{ATP} (0.06 ± 0.02 nA) and GFP (0.07 ± 0.02 nA; Fig. 6*B*). In K_{ATP} + TRPM4, large TRPM4-like currents

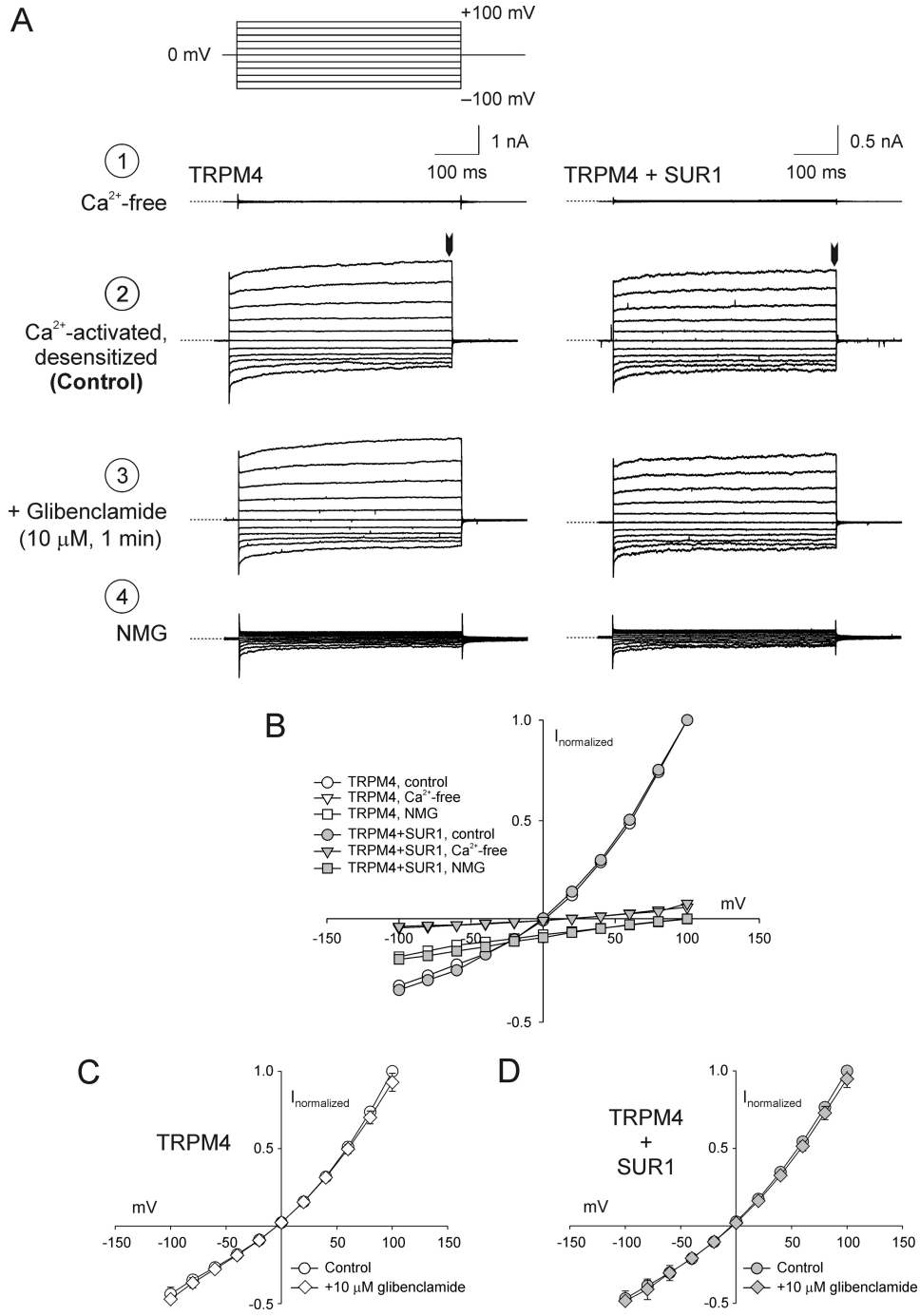

FIGURE 3. **Voltage dependence of TRPM4 current properties is not modified by SUR1 or glibenclamide.** *A*, currents measured in excised patches from representative cells transfected with TRPM4 (*left*) or TRPM4 and SUR1 (*right*). Data were acquired sequentially upon excision in a Ca^{2+}-free Na^{+} buffer (*background*) (*1*); at the steady-state after desensitization of the currents activated by 300 μM Ca^{2+} (*control*) (*2*); following 1-min exposure to 10 μM glibenclamide (*3*); and after replacement of Na^{+} with NMG (*4*). The composition of the bath solutions is the same as described in the legend to Fig. 2. The pulse protocol is shown in the *top left panel*. The *dotted lines* indicate zero current. *B*, current-voltage relationships of background (*triangles*), steady-state Ca^{2+}-activated (*circles*), and NMG-inhibited (*squares*) currents, from the same individual experiments as described in *A*. Currents at each voltage were measured at the end of the 500-ms pulse and are normalized to the current measured at +100 mV in control conditions (indicated by *arrowheads* in *A*, *panel 2*), *i.e.* 2.5 nA in TRPM4 and 1.5 nA in TRPM4 + SUR1. *C* and *D*, voltage dependence of steady-state currents in cells transfected with TRPM4 (*C*) or TRPM4 + SUR1 (*D*), before and after exposure to 10 μM glibenclamide, from experiments as described in *A*. Data are means ± S.E. from seven patches per transfection type, and in each experiment, currents were normalized to their own control at +100 mV. On average, control currents at +100 mV were 2.2 ± 0.8 nA (TRPM4) and 1.7 ± 0.5 (TRPM4 + SUR1) (non-significant, $p = 0.54$; unpaired Student's *t* test).

were activated that peaked at 3.5 ± 0.8 nA, relaxed to the steady-state (2.5 ± 0.6 nA, Fig. 6*B*), and were inactivated in the absence of Ca^{2+} with kinetics in the same range as those described in the legends to Figs. 2 and 4. Despite the presence of SUR1 subunits, as evidenced by the formation of functional K_{ATP} channels, the TRPM4-like currents in K_{ATP} + TRPM4 patches were not inhibited by tolbutamide (Fig. 6*B*), consistent with the hypothesis that SUR1 does not

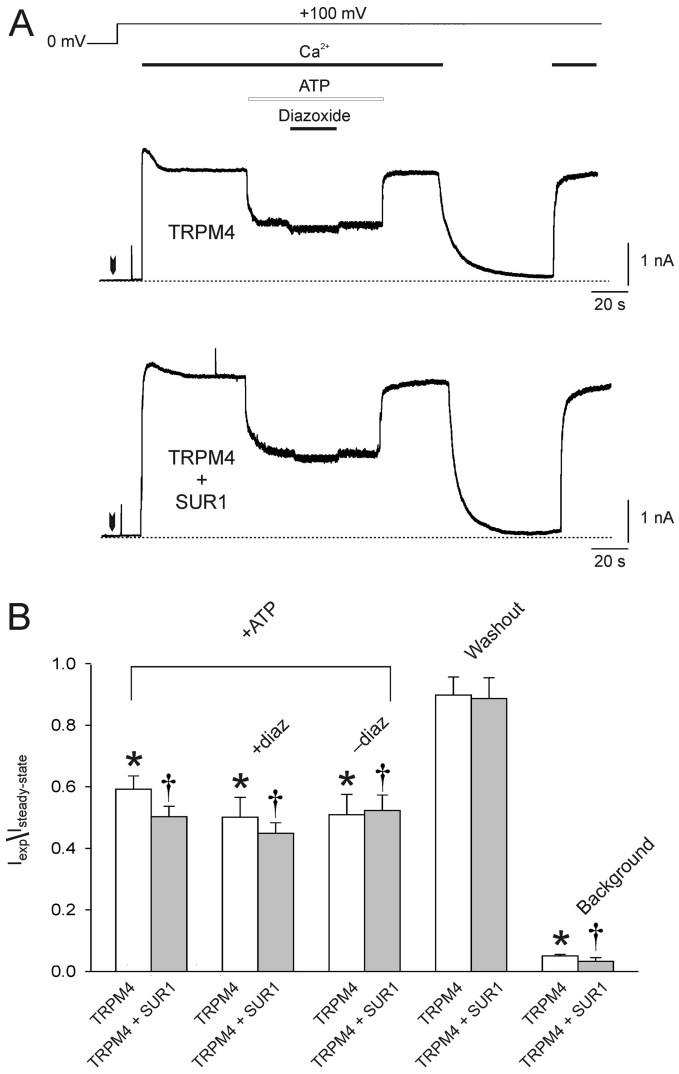

FIGURE 4. **Currents in TRPM4 and TRPM4 + SUR1 inside-out patches are inhibited by ATP to a similar extent, and diazoxide does not reverse this inhibition.** *A*, representative current traces. V_m was first held at 0 mV, and patches were excised into Na^+-EGTA buffer containing 150 mM NaCl, 5 mM EGTA, and 10 mM Hepes, plus 500 μM free Mg^{2+}. *Arrowheads* mark the point of excision; *dotted lines* indicate zero current. V_m was then stepped to +100 mV, and subsequently, the patches were exposed to Na^+-EGTA with 300 μM free Ca^{2+}. Once the Ca^{2+}-activated currents had relaxed to the steady-state, the patches were exposed to 10 μM free ATP, first in the absence, then in the presence, and finally in the absence of 250 μM diazoxide. Recovery from inhibition was assessed by returning the patches to ATP-free buffer, and background currents were obtained by exposure to Ca^{2+}-free buffer. The appropriate amounts of $MgCl_2$, $CaCl_2$, and K^+-ATP to be added in each bath solution to attain the desired free concentrations of Mg^{2+}, Ca^{2+}, and ATP were calculated by means of the CaBuf program. *B*, currents measured in the different experimental situations, normalized to the steady-state current ($I_{exp}/I_{steady\text{-}state}$). *diaz*, diazoxide; *washout*, currents measured after removal of ATP; *background*, currents measured after exposure to Ca^{2+}-free buffer. Data are means ± S.E. from 6 measurements. * and †, $p < 0.05$ as compared with $I_{steady\text{-}state}$ in TRPM4 and TRPM4 + SUR1, respectively (paired Student's *t* test). On average, $I_{steady\text{-}state}$ was 87 ± 4% (TRPM4) and 84 ± 4% (TRPM4 + SUR1) of the peak current, respectively 4.3 ± 0.6 nA and 4.7 ± 0.3 nA. No significant differences were found between TRPM4 and TRPM4 + SUR1 for any of the parameters studied ($p = 0.1–0.9$; unpaired Student's *t* test).

modulate TRPM4 channels. To highlight this fact, individual current measurements taken before and after exposure to the drug in the same experiment have been represented in Fig. 6*B* with the same symbol, in *light* and *dark* shades of *gray*, respectively.

FRET Provides No Evidence for Structural Association between TRPM4 and SUR1—In cells cotransfected with TRPM4 and SUR1, the properties of TRPM4-mediated currents were not modified by drugs that have been shown to target SUR1 (Figs. 2–4 and 6), and this strongly suggests that SUR1 does not functionally modulate TRPM4 channel activity in this system. To further evaluate the possibility of a physical interaction between TRPM4 and SUR1, we performed FRET analyses; results are summarized in the legend to Fig. 7. The fluorophore-tagged proteins used in these studies were functionally indistinguishable from those used in electrophysiological and radiotracer efflux experiments (Figs. 2–6). Thus, the kinetic properties of TRPM4-mediated Na^+ currents in cells expressing TRPM4-ECFP or TRPM4-EYFP were identical to those of TRPM4-EGFP (supplemental Fig. S1), and cotransfection of Kir6.2-ECFP and SUR1-EYFP resulted in the assembly of functional K_{ATP} channels (supplemental Fig. S2). Fluorescence spectra (Fig. 7, *A* and *B*) demonstrate FRET coupling between TRPM4-ECFP and TRPM4-EYFP, as well as between Kir6.2-ECFP and SUR1-EYFP, confirming that TRPM4 subunits form a channel complex, as do Kir6.2 and SUR1. Thus, the apparent FRET efficiency of fluorophore pair TRPM4-ECFP/TRPM4-EYFP was ~28%, similar to that of Kir6.2-ECFP/SUR1-EYFP and 3-fold higher than that observed in COSm6 cells expressing EYFP-only constructs, which results from the unspecific excitation of EYFP at 430 nm (Fig. 7*C*). However, there was no detectable FRET between TRPM4-ECFP and SUR1-EYFP (Fig. 7*C*). Thus, these data also provide no evidence for physical association between TRPM4 and SUR1.

DISCUSSION

Sulfonylurea receptor subunits (*e.g.* SUR1) couple to inward-rectifying K^+ channel subunits (*e.g.* Kir6.2) to form ATP-sensitive K^+ (K_{ATP}) channels (Fig. 1), which are central to numerous physiological processes, from insulin secretion to the generation and maintenance of cardiac rhythm and vascular tone (26). The archetypal pancreatic β-cell K_{ATP} channel, for example, is composed of four Kir6.2 and four SUR1 subunits (27), and the link between these two proteins has proven essential for K_{ATP} channel gating, modulation, and pharmacology (25, 28, 29). In the K_{ATP} channel octamer, the Kir6.*x* subunits define the ATP-sensitive pore, whereas the SUR*x* subunits confer sensitivity to sulfonylureas, K^+ channel openers, and NDPs (7). Only the fully assembled octameric channel complex can reach the plasma membrane, as SUR1 and Kir6.2 contain endoplasmic reticulum retention motifs that must be shielded mutually to allow trafficking (30). This tight and required structural and functional association also seems to be exclusive; whereas one report suggested that SUR1 is capable of coupling with Kir1.1 (8), these findings have not been confirmed by independent research, and Kir1.1 subunits are well known to assemble in fully functional tetrameric channels, indispensable to the regulation of ion homeostasis in the kidney (31).

TRPM4 subunits are distantly related members of the cation channel superfamily that also assemble into tetrameric functional channels (Fig. 1) (32) which are constitutively expressed in vascular smooth muscle, pacemaker cells, mast cells, and lymphocytes and play key roles in vasoconstriction, cerebral

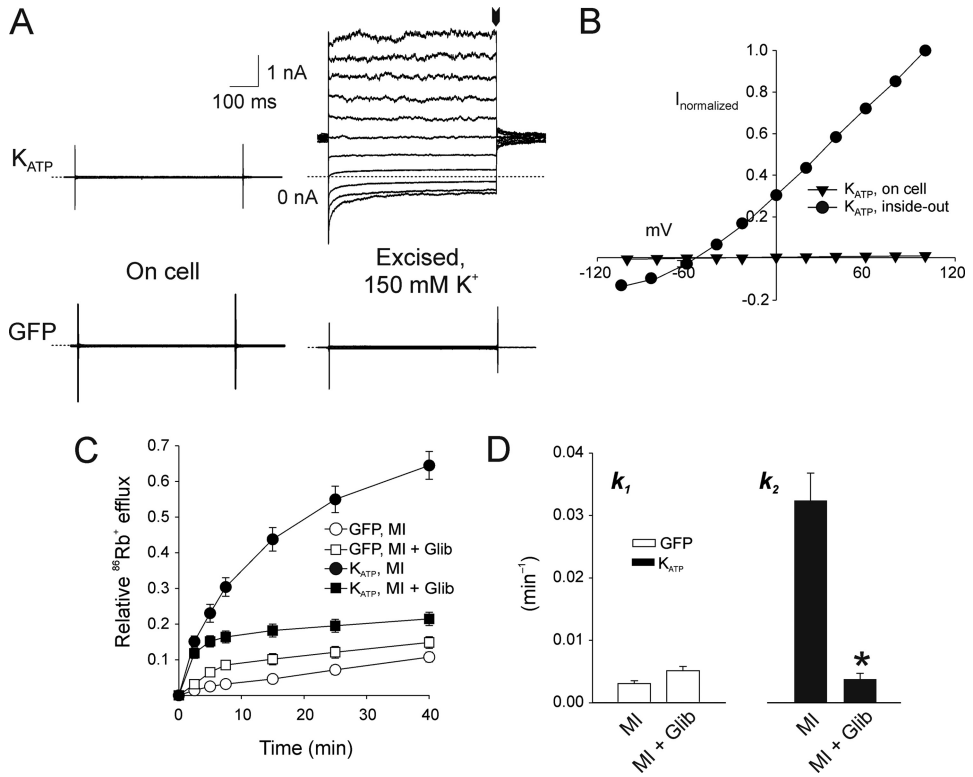

FIGURE 5. **Cotransfection of SUR1 with Kir6.2 results in functional $K_{\Delta TP}$ channels.** *A*, currents measured in a representative cell cotransfected with Kir6.2 and the same SUR1 plasmid DNA used in the experiments shown in Figs. 2–4 (*top panels*) or in a representative mock-transfected cell (*GFP*; *bottom*); on cell (*left*) and after excision into a K^+ buffer (K^+) containing 150 mM KCl, 1 mM K^+-EDTA, 1 mM EGTA, and 10 mM Hepes (pH 7.4 with KOH) (*right*). The pulse protocol is the same as in Fig. 3*A*. The *dotted lines* indicate zero current. *B*, voltage dependence of currents measured on cell (*triangles*) and in inside-out excised patches (*circles*), from experiments in K_{ATP}-expressing cells as in *A*. Currents at each voltage were measured at the end of the 500-ms pulse and are normalized to the current measured at +100 mV in the excised patch configuration (indicated by an *arrowhead* in the *top right panel* of *A*) on average 3.6 ± 0.8 nA. Data are means ± S.E. from five patches. *C*, time course of $^{86}Rb^+$ efflux in mock-transfected cells (*GFP*; *white symbols*) or in cells cotransfected with Kir6.2 and SUR1 (K_{ATP}; *black symbols*) under metabolic inhibition conditions, in absence (*MI*, *circles*) or presence of 10 μM glibenclamide (*MI + Glib*; *squares*). *D*, flux data were fit to Equation 1 to estimate the rate constants for K_{ATP}-dependent $^{86}Rb^+$ efflux k_2 (*black bars*). *, $p < 0.05$ as compared with k_2 in the absence of glibenclamide (paired Student's *t* test). Nonspecific k_1 (*white bars*) were estimated from GFP-transfected cells. *C* and *D*, results are means ± S.E. from four to six experiments.

blood flow, the generation of heart rhythm, and the immune response (33–39). TRPM4-mediated currents are up-regulated in cardiomyocytes from spontaneous hypertensive rats (40), and gain-of-function mutations in TRPM4 have been associated with familial heart disease (41, 42). TRPM4 channel kinetics are finely tuned by diverse cellular factors, including Ca^{2+}-calmodulin, adenine nucleotides, and phosphoinositide 4,5-bisphosphate (15).

Several recent studies have led to the suggestion that SUR1 may also couple with TRPM4 to form novel channels critical to the outcome of injuries to the central nervous system In particular, it has been postulated that *de novo* expression of a putative TRPM4/SUR1 channel complex in neurovascular tissues after traumatic brain injury, spinal cord injury, ischemic stroke, or brain aneurysm is responsible for the dramatic up-regulation of cationic currents that lead to microvascular failure and cerebral edema, often with devastating consequences (9). Accordingly, expression of SUR1 is up-regulated in reactive astrocytes, neurons, and capillaries of rodent models for ischemia, traumatic brain injury, and spinal cord injury (11, 12, 43–45). The effects of trauma appear to be reduced by administration of glibenclamide (46, 47); clinical trials to test the potential of this antidiabetic drug as a treatment for brain edema are under way (48), but the subject remains controversial (49, 50). On the other hand, fragmentation and hemorrhaging in capillaries correlate with an increase in TRPM4 expression in rats after spinal cord injury and are significantly mitigated in TRPM4-null mice (17).

Although these studies provide very provocative interpretations, the TRPM4-SUR1 association hypothesis remains untested experimentally. Therefore, we performed functional and structural studies in COSm6 cells expressing TRPM4 in the absence and presence of SUR1 (Figs. 2–7). Na^+ currents measured in excised inside-out patches from cells transfected with TRPM4 were 1) activated by cytoplasmic Ca^{2+} (Figs. 2, 4, and 6); 2) voltage-dependent and outward-rectifying (Fig. 3); 3) reversibly inhibited by ATP (Fig. 4); and 4) underwent desensitization (Figs. 2, 4, and 6). These were in agreement with the biophysical properties of TRPM4 channels established by several independent groups (15, 16) and were not modified by the presence of SUR1 (Figs. 2–4 and 6). Co-expression with SUR1 did not confer sensitivity to glibenclamide, tolbutamide, or diazoxide (Figs. 2, 4, and 6). When coexpressed with Kir6.2, the same SUR1 subunits assembled in fully functional, glibenclamide-sensitive K_{ATP} channels (Fig. 5) that were not affected by the presence of TRPM4 (Fig. 6). FRET analysis confirmed the strong physical association between TRPM4 subunits and between Kir6.2 and SUR1 subunits, while showing no evidence for the structural coupling of TRPM4 and SUR1 (Fig. 7).

Our data thus strongly suggest that either functional or physical interaction between TRPM4 and SUR1 is improbable.

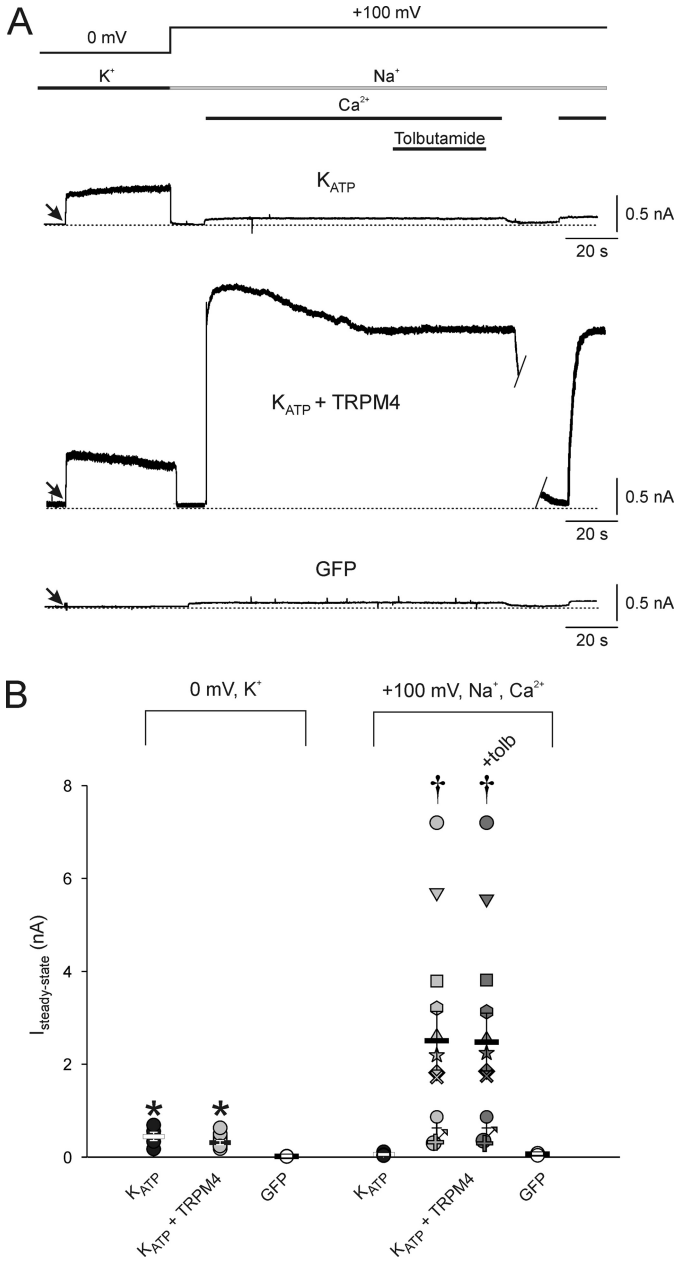

FIGURE 6. **In the same cells, SUR1 modulates the activity of K_{ATP} channels but does not affect TRPM4 currents.** *A*, continuous current traces in inside-out excised patches from representative cells cotransfected with Kir6.2 and SUR1 (K_{ATP}), Kir6.2, SUR1, and TRPM4 (K_{ATP} + TRPM4), or mock-transfected (*GFP*). V_m was first held at 0 mV, and patches were excised into K^+ buffer (composition as in Fig. 5). *Arrows* mark the point of excision; *dotted lines* indicate zero current. Subsequently, V_m was stepped to +100 mV, and patches were exposed to Na^+ buffer in absence or presence of 300 μM Ca^{2+} (composition as in Fig. 2). At selected times, the effect of 200 μM tolbutamide was tested. *B*, summary of steady-state currents ($I_{steady\text{-}state}$) measured in the conditions indicated on top of the data sets, from experiments as in *A*. *Symbols* represent data from individual patches (n = 5–12); *bars* indicate the means ± S.E. of all experiments. In columns 5 and 6, the same symbol is used to represent the currents in the absence (*light gray*) or presence (*dark gray*) of tolbutamide (*tolb*) from the same experiment. * and †, $p < 0.05$ as compared with the mock-transfected cells in 0 mV, K^+ conditions, and in +100 mV, Na^+, Ca^{2+} conditions, respectively (one-way analysis of variance and Kruskal-Wallis test).

Structurally such association seems unlikely because SUR1 probably packs tightly against the two inner helices of the Kir6.2 subunit (51), whereas the S1–S4 "voltage sensor" domain (52) will likely pack against the inner helices in TRPM4 (Fig. 1).

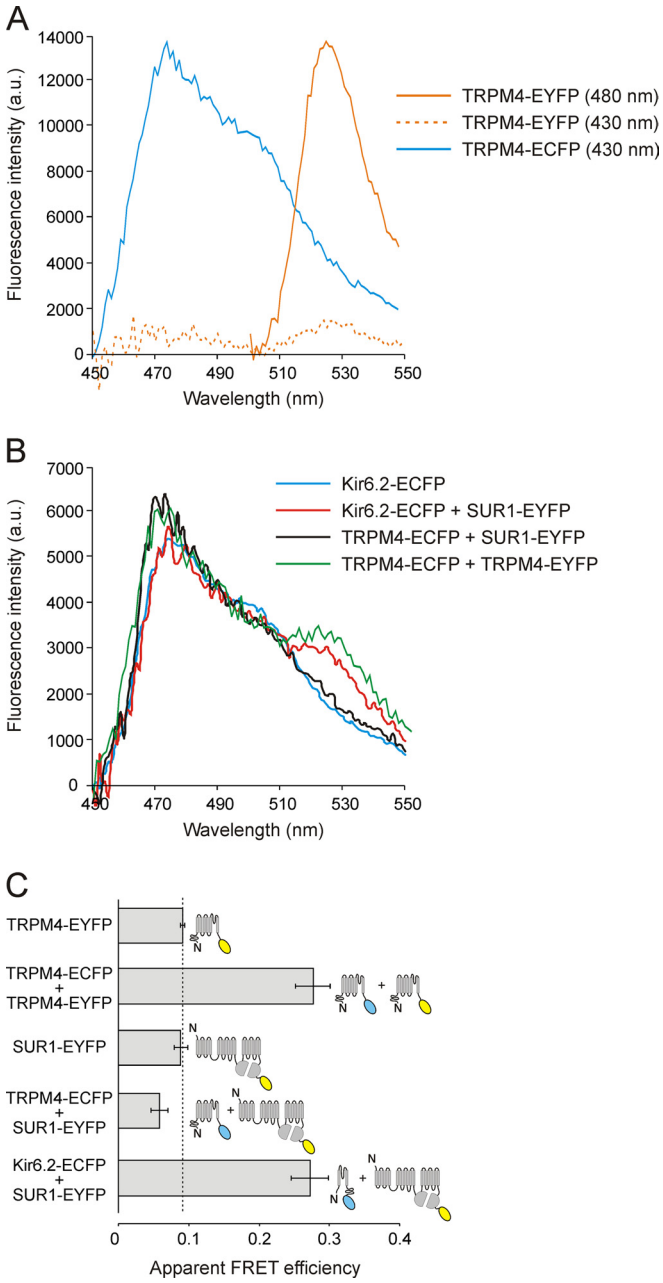

FIGURE 7. **FRET analysis demonstrates no structural association between TRPM4 and SUR1.** *A*, representative emission spectra from COSm6 cells transfected with TRPM4-EYFP or TRPM4-ECFP. Cells expressing TRPM4-EYFP were excited at 480 nm (*solid orange line*) or 430 nm (*dashed orange line*), and emission between 490–550 and 450–550 nm, respectively, was measured by means of fluorescence spectroscopy. Cells expressing TRPM4-ECFP were excited at 430 nm, and emission between 450–550 nm was measured (*cyan*). *B*, representative emission spectra from cells expressing Kir6.2, TRPM4, and SUR1 with C-terminal ECFP or EYFP tags. Cells were excited at 430 nm, and emission between 450–550 nm was measured. A remarkable emission peak at 525 nm, which is due to ECFP/EYFP FRET, was detected in cells cotransfected with Kir6.2-ECFP plus SUR1-EYFP (*red*) or TRPM4-ECFP plus TRPM4-EYFP (*green*), but not for those cotransfected with TRPM4-ECFP plus SUR1-EYFP (*black*) or Kir6.2-ECFP (*cyan*). *C*, apparent FRET efficiencies between the C-terminal ECFP and EYFP tags of Kir6.2, TRPM4, and SUR1. The apparent FRET efficiency due to the unspecific excitation of EYFP was 0.09 ± 0.003 in cells transfected with TRPM4-EYFP and 0.09 ± 0.001 in cells transfected with SUR1-EYFP. Coexpression of TRPM4-ECFP and TRPM4-EYFP, or Kir6.2-ECFP and SUR1-EYFP, resulted in apparent FRET efficiencies of 0.28 ± 0.03 and 0.27 ± 0.03, respectively. In cells cotransfected with TRPM4-ECFP and SUR1-EYFP, the apparent FRET efficiency was 0.06 ± 0.01, *i.e.* within in the range of that measured in cells transfected with EYFP fusion constructs alone. FRET data are presented as mean ± S.E. from three to six measurements, each from an independent transfection. a.u., arbitrary units.

Here, we used the long splice variant of TRPM4, but other variants have been identified that lack different portions of the N terminus (16). In most, however, the transmembrane segments remain intact (22, 23, 53) and thus are likely to undergo similar packing to the full-length protein and hence still unlikely to physically couple to SUR1. The TRPM4 mRNA detected in neurovascular cells of rodents subjected to spinal cord injury is actually equivalent to the long splice variant (17), and this suggests that shorter orthologs are not likely to play a relevant role. We provide compelling evidence that in a recombinant system, TRPM4 channels are not modulated by SUR1; although we cannot discard the possibility that interaction may occur in a different cellular environment, our data do not support the hypothesis that the cationic currents measured in astrocytes and endothelial cells from rodent models for neurovascular trauma are due to TRPM4 channels under direct modulation by SUR1 subunits (9). At the foundation of this hypothesis lies the observation that these currents are apparently inhibited by sulfonylureas (11, 12, 45, 54). It is unclear whether the effect of these drugs was tested once desensitization of TRPM4-like currents was complete and a steady-state had been reached, as done in our study (Figs. 2, 4, and 6) and essential to prevent artifacts due to ongoing inactivation (23, 55–57). One possibility is that both TRPM4 and K_{ATP} channels are up-regulated at the site of injury and contribute to different aspects of the pathogenesis of brain edema and microvascular failure. TRPM4-mediated currents are known to be up-regulated in certain pathological situations (40–42), and it is thus plausible that TRPM4 channels are responsible for the cationic currents that lead to post-traumatic neurovascular cell swelling and necrosis. On the other hand, Kir6.1 and Kir6.2 subunits are abundant in tissues where SUR1 is up-regulated following a stroke (54), and the possible concomitant increase in K_{ATP} currents remains to be addressed.

Acknowledgments—We thank Simonne Francis for technical assistance. mTRPM4b in pEGFP-N1 was a kind gift from J. Marc Simard (University of Maryland School of Medicine, Baltimore, MD).

REFERENCES

1. Hille, B. (2001) *Ion Channels of Excitable Membranes*, 3rd Ed., pp. 237–268, Sinauer Associates Inc., Sunderland, MA
2. Venkatachalam, K., and Montell, C. (2007) TRP channels. *Annu. Rev. Biochem.* **76,** 387–417
3. Zhu, Z., Luo, Z., Ma, S., and Liu, D. (2011) TRP channels and their implications in metabolic diseases. *Pflugers Arch.* **461,** 211–223
4. Voets, T., and Nilius, B. (2007) Modulation of TRPs by PIPs. *J. Physiol.* **582,** 939–944
5. Locher, K. P. (2009) Review. Structure and mechanism of ATP-binding cassette transporters. *Philos. Trans. R Soc. Lond. B Biol. Sci.* **364,** 239–245
6. Muallem, D., and Vergani, P. (2009) Review. ATP hydrolysis-driven gating in cystic fibrosis transmembrane conductance regulator. *Philos. Trans. R Soc. Lond. B Biol. Sci.* **364,** 247–255
7. Nichols, C. G. (2006) KATP channels as molecular sensors of cellular metabolism. *Nature* **440,** 470–476
8. Ammälä, C., Moorhouse, A., Gribble, F., Ashfield, R., Proks, P., Smith, P. A., Sakura, H., Coles, B., Ashcroft, S. J., and Ashcroft, F. M. (1996) Promiscuous coupling between the sulphonylurea receptor and inwardly rectifying potassium channels. *Nature* **379,** 545–548
9. Simard, J. M., Kahle, K. T., and Gerzanich, V. (2010) Molecular mechanisms of microvascular failure in central nervous system injury–synergistic roles of NKCC1 and SUR1/TRPM4. *J. Neurosurg.* **113,** 622–629
10. Nilius, B., Prenen, J., Voets, T., and Droogmans, G. (2004) Intracellular nucleotides and polyamines inhibit the Ca^{2+}-activated cation channel TRPM4b. *Pflugers Arch.* **448,** 70–75
11. Chen, M., Dong, Y., and Simard, J. M. (2003) Functional coupling between sulfonylurea receptor type 1 and a nonselective cation channel in reactive astrocytes from adult rat brain. *J. Neurosci.* **23,** 8568–8577
12. Simard, J. M., Tsymbalyuk, O., Ivanov, A., Ivanova, S., Bhatta, S., Geng, Z., Woo, S. K., and Gerzanich, V. (2007) Endothelial sulfonylurea receptor 1-regulated NC Ca-ATP channels mediate progressive hemorrhagic necrosis following spinal cord injury. *J. Clin. Invest.* **117,** 2105–2113
13. Simard, J. M., Tarasov, K. V., and Gerzanich, V. (2007) Non-selective cation channels, transient receptor potential channels and ischemic stroke. *Biochim. Biophys. Acta* **1772,** 947–957
14. Chen, M., and Simard, J. M. (2001) Cell swelling and a nonselective cation channel regulated by internal Ca^{2+} and ATP in native reactive astrocytes from adult rat brain. *J. Neurosci.* **21,** 6512–6521
15. Guinamard, R., Sallé, L., and Simard, C. (2011) The non-selective monovalent cationic channels TRPM4 and TRPM5. *Adv. Exp. Med. Biol.* **704,** 147–171
16. Vennekens, R., and Nilius, B. (2007) Insights into TRPM4 function, regulation and physiological role. *Handb. Exp. Pharmacol.* **179,** 269–285
17. Gerzanich, V., Woo, S. K., Vennekens, R., Tsymbalyuk, O., Ivanova, S., Ivanov, A., Geng, Z., Chen, Z., Nilius, B., Flockerzi, V., Freichel, M., and Simard, J. M. (2009) *De novo* expression of Trpm4 initiates secondary hemorrhage in spinal cord injury. *Nat. Med.* **15,** 185–191
18. Simard, J. M., Woo, S. K., Norenberg, M. D., Tosun, C., Chen, Z., Ivanova, S., Tsymbalyuk, O., Bryan, J., Landsman, D., and Gerzanich, V. (2010) Brief suppression of Abcc8 prevents autodestruction of spinal cord after trauma. *Sci. Transl. Med.* **2,** 28ra29
19. Sala-Rabanal, M., Kucheryavykh, L. Y., Skatchkov, S. N., Eaton, M. J., and Nichols, C. G. (2010) Molecular mechanisms of EAST/SeSAME syndrome mutations in Kir4.1 (KCNJ10). *J. Biol. Chem.* **285,** 36040–36048
20. Makhina, E. N., and Nichols, C. G. (1998) Independent trafficking of KATP channel subunits to the plasma membrane. *J. Biol. Chem.* **273,** 3369–3374
21. Makhina, E. N., and Nichols, C. G. (2001) Mutant GFP- Based FRET Analysis of K^+ Channel Organization in *Ion Channel Localization Methods and Protocols*, pp. 261–274, Humana Press, Inc., Totowa, NJ
22. Launay, P., Fleig, A., Perraud, A. L., Scharenberg, A. M., Penner, R., and Kinet, J. P. (2002) TRPM4 is a Ca^{2+}-activated nonselective cation channel mediating cell membrane depolarization. *Cell* **109,** 397–407
23. Nilius, B., Prenen, J., Droogmans, G., Voets, T., Vennekens, R., Freichel, M., Wissenbach, U., and Flockerzi, V. (2003) Voltage dependence of the Ca^{2+}-activated cation channel TRPM4. *J. Biol. Chem.* **278,** 30813–30820
24. Gribble, F. M., Ashfield, R., Ammälä, C., and Ashcroft, F. M. (1997) Properties of cloned ATP-sensitive K^+ currents expressed in *Xenopus* oocytes. *J. Physiol.* **498**, 87–98
25. Koster, J. C., Sha, Q., and Nichols, C. G. (1999) Sulfonylurea and K^+-channel opener sensitivity of K-ATP channels. Functional coupling of Kir6.2 and SUR1 subunits. *J. Gen. Physiol.* **114,** 203–213
26. Akrouh, A., Halcomb, S. E., Nichols, C. G., and Sala-Rabanal, M. (2009) Molecular biology of K-ATP channels and implications for health and disease. *IUBMB Life* **61,** 971–978
27. Shyng, S., and Nichols, C. G. (1997) Octameric stoichiometry of the KATP channel complex. *J. Gen. Physiol.* **110,** 655–664
28. Kuhner, P., Prager, R., Stephan, D., Russ, U., Winkler, M., Ortiz, D., Bryan, J., and Quast, U. (2011) Importance of the Kir6.2 N terminus for the interaction of glibenclamide and repaglinide with the pancreatic K_{ATP} channel. *Naunyn. Schmiedebergs Arch. Pharmacol.* DOI: 10.1007/s00210-011-0709-8
29. Pratt, E. B., Tewson, P., Bruederle, C. E., Skach, W. R., and Shyng, S. L. (2011) N-terminal transmembrane domain of SUR1 controls gating of Kir6.2 by modulating channel sensitivity to PIP_2. *J. Gen. Physiol.* **137,** 299–314
30. Zerangue, N., Schwappach, B., Jan, Y. N., and Jan, L. Y. (1999) A new ER

trafficking signal regulates the subunit stoichiometry of plasma membrane K(ATP) channels. *Neuron* **22,** 537–548
31. Hibino, H., Inanobe, A., Furutani, K., Murakami, S., Findlay, I., and Kurachi, Y. (2010) Inwardly rectifying potassium channels: Their structure, function, and physiological roles. *Physiol. Rev.* **90,** 291–366
32. Murakami, M., Xu, F., Miyoshi, I., Sato, E., Ono, K., and Iijima, T. (2003) Identification and characterization of the murine TRPM4 channel. *Biochem. Biophys. Res. Commun.* **307,** 522–528
33. Crnich, R., Amberg, G. C., Leo, M. D., Gonzales, A. L., Tamkun, M. M., Jaggar, J. H., and Earley, S. (2010) Vasoconstriction resulting from dynamic membrane trafficking of TRPM4 in vascular smooth muscle cells. *Am. J. Physiol. Cell Physiol.* **299,** C682–694
34. Demion, M., Bois, P., Launay, P., and Guinamard, R. (2007) TRPM4, a Ca^{2+}-activated nonselective cation channel in mouse sino-atrial node cells. *Cardiovasc. Res.* **73,** 531–538
35. Earley, S., Straub, S. V., and Brayden, J. E. (2007) Protein kinase C regulates vascular myogenic tone through activation of TRPM4. *Am. J. Physiol. Heart Circ. Physiol.* **292,** H2613–2622
36. Launay, P., Cheng, H., Srivatsan, S., Penner, R., Fleig, A., and Kinet, J. P. (2004) TRPM4 regulates calcium oscillations after T cell activation. *Science* **306,** 1374–1377
37. Morita, H., Honda, A., Inoue, R., Ito, Y., Abe, K., Nelson, M. T., and Brayden, J. E. (2007) Membrane stretch-induced activation of a TRPM4-like nonselective cation channel in cerebral artery myocytes. *J. Pharmacol. Sci.* **103,** 417–426
38. Reading, S. A., and Brayden, J. E. (2007) Central role of TRPM4 channels in cerebral blood flow regulation. *Stroke* **38,** 2322–2328
39. Shimizu, T., Owsianik, G., Freichel, M., Flockerzi, V., Nilius, B., and Vennekens, R. (2009) TRPM4 regulates migration of mast cells in mice. *Cell Calcium* **45,** 226–232
40. Guinamard, R., Demion, M., Magaud, C., Potreau, D., and Bois, P. (2006) Functional expression of the TRPM4 cationic current in ventricular cardiomyocytes from spontaneously hypertensive rats. *Hypertension* **48,** 587–594
41. Kruse, M., Schulze-Bahr, E., Corfield, V., Beckmann, A., Stallmeyer, B., Kurtbay, G., Ohmert, I., Schulze-Bahr, E., Brink, P., and Pongs, O. (2009) Impaired endocytosis of the ion channel TRPM4 is associated with human progressive familial heart block type I. *J. Clin. Invest.* **119,** 2737–2744
42. Liu, H., El Zein, L., Kruse, M., Guinamard, R., Beckmann, A., Bozio, A., Kurtbay, G., Mégarbané, A., Ohmert, I., Blaysat, G., Villain, E., Pongs, O., and Bouvagnet, P. (2010) Gain-of-function mutations in TRPM4 cause autosomal dominant isolated cardiac conduction disease. *Circ. Cardiovasc. Genet.* **3,** 374–385
43. Simard, J. M., and Chen, M. (2004) Regulation by sulfanylurea receptor type 1 of a non-selective cation channel involved in cytotoxic edema of reactive astrocytes. *J. Neurosurg. Anesthesiol.* **16,** 98–99
44. Simard, J. M., Kilbourne, M., Tsymbalyuk, O., Tosun, C., Caridi, J., Ivanova, S., Keledjian, K., Bochicchio, G., and Gerzanich, V. (2009) Key role of sulfonylurea receptor 1 in progressive secondary hemorrhage after brain contusion. *J. Neurotrauma* **26,** 2257–2267
45. Woo, S. K., Kwon, M. S., Geng, Z., Chen, Z., Ivanov, A., Bhatta, S., Gerzanich, V., and Simard, J. M. (2011) Sequential activation of hypoxia-inducible factor I and specificity protein I is required for hypoxia-induced transcriptional stimulation of ABCC8. *J. Cereb. Blood Flow Metab.* DOI:10.1038/jcbfm.2011.159
46. Patel, A. D., Gerzanich, V., Geng, Z., and Simard, J. M. (2010) Glibenclamide reduces hippocampal injury and preserves rapid spatial learning in a model of traumatic brain injury. *J. Neuropathol. Exp. Neurol.* **69,** 1177–1190
47. Popovich, P. G., Lemeshow, S., Gensel, J. C., and Tovar, C. A. (2010) Independent evaluation of the effects of glibenclamide on reducing progressive hemorrhagic microsis after cervical spinal cord injury. *Exp. Neurol.* **232,** 615–622
48. Walcott, B. P., Kahle, K. T., and Simard, J. M. (2011) Novel treatment targets for cerebral edema. *Neurotherapeutics* **9,** 65–72
49. Favilla, C. G., Mullen, M. T., Ali, M., Higgins, P., and Kasner, S. E. (2011) Sulfonylurea use before stroke does not influence outcome. *Stroke* **42,** 710–715
50. Simard, J. M., Kent, T. A., and Kunte, H. (2011) Letter by Simard *et al* regarding article, "Sulfonylurea use before stroke does not influence outcome." *Stroke* **42,** e409
51. Mikhailov, M. V., Campbell, J. D., de Wet, H., Shimomura, K., Zadek, B., Collins, R. F., Sansom, M. S., Ford, R. C., and Ashcroft, F. M. (2005) 3-D structural and functional characterization of the purified KATP channel complex Kir6.2-SUR1. *EMBO J.* **24,** 4166–4175
52. Long, S. B., Campbell, E. B., and Mackinnon, R. (2005) Voltage sensor of Kv1.2: Structural basis of electromechanical coupling. *Science* **309,** 903–908
53. Xu, X. Z., Moebius, F., Gill, D. L., and Montell, C. (2001) Regulation of melastatin, a TRP-related protein, through interaction with a cytoplasmic isoform. *Proc. Natl. Acad. Sci. U.S.A.* **98,** 10692–10697
54. Simard, J. M., Chen, M., Tarasov, K. V., Bhatta, S., Ivanova, S., Melnitchenko, L., Tsymbalyuk, N., West, G. A., and Gerzanich, V. (2006) Newly expressed SUR1-regulated NC(Ca-ATP) channel mediates cerebral edema after ischemic stroke. *Nat Med* **12,** 433–440
55. Nilius, B., Prenen, J., Janssens, A., Owsianik, G., Wang, C., Zhu, M. X., and Voets, T. (2005) The selectivity filter of the cation channel TRPM4. *J. Biol. Chem.* **280,** 22899–22906
56. Nilius, B., Prenen, J., Tang, J., Wang, C., Owsianik, G., Janssens, A., Voets, T., and Zhu, M. X. (2005) Regulation of the Ca^{2+} sensitivity of the nonselective cation channel TRPM4. *J. Biol. Chem.* **280,** 6423–6433
57. Zhang, Z., Okawa, H., Wang, Y., and Liman, E. R. (2005) Phosphatidylinositol 4,5-bisphosphate rescues TRPM4 channels from desensitization. *J. Biol. Chem.* **280,** 39185–39192